

ARTICLE OPEN



CHEK2 loss endows chemotherapy resistance to hematopoietic stem cells

Jing Zhou¹, Tianyuan Hu², Dian Li¹, Sanming Li⁴, Minhua Li¹, Xiangguo Shi^{2,5} and Daisuke Nakada^{1,2}✉

© The Author(s) 2025

Individuals with history of chemo- or radiotherapy frequently exhibit somatic mosaicism in the blood, often involving mutations in genes responsible for DNA damage responses (DDR), such as *CHEK2*. However, the mechanisms by which *CHEK2* mutations promote the expansion of mutant cells following chemo- or radiotherapy remain poorly understood. Here, we demonstrate that loss of *CHEK2* confers resistance to chemotherapy in hematopoietic stem and progenitor cells (HSPCs). Through a CRISPR-based screen, we identified *CHEK2* as a gene whose loss enhances resistance to cytotoxic chemotherapies. A complementary drug screen revealed that *CHEK2*-mutant cells are also resistant to DNA hypomethylating agents. *Chek2*-deficient HSPCs persist in vivo following chemotherapy exposure and exhibit elevated levels of DNA damage compared to wild-type cells. Our findings establish that *CHEK2* loss promotes chemoresistance in HSPCs, offering new insights into the role of *CHEK2* in therapy-related clonal hematopoiesis observed in cancer patients.

Leukemia; <https://doi.org/10.1038/s41375-025-02850-w>

INTRODUCTION

Accrual of somatic mutations becomes prevalent in multiple tissues with age. Clonal hematopoiesis (CH) refers to somatic mosaicism in the blood system wherein mutations in genes such as *DNMT3A*, *TET2*, and *ASXL1* are found increasing with age in healthy individuals [1, 2]. CH not only elevates the risk of hematologic malignancies but is also associated with a range of age- and inflammation-related disorders, including cardiovascular, liver, and kidney diseases. The risk of these conditions correlates with the variant allele frequency (VAF) of CH, supporting the idea that mutant hematopoietic cells act as a reservoir for further mutagenesis and contribute to systemic inflammation.

The fitness of CH clones is shaped by environmental factors such as inflammation, smoking, and chemotherapy [3]. These factors apply selective pressure favoring specific mutations: for instance, inflammation tends to select for *DNMT3A* or *TET2* mutations, while smoking is associated with *ASXL1*-mutant CHIP [4–7]. In cancer patients with prior chemotherapy exposure, blood samples are often enriched for mutations in DNA damage response (DDR) genes such as *TP53*, *PPM1D*, and *CHEK2* [8–12]. This phenomenon, known as therapy-related CH (t-CH), illustrates how environmental stressors can drive the selection of particular mutational profiles [13].

The DDR pathway orchestrates cellular responses to DNA damage, preserving genomic integrity and suppressing tumorigenesis [14]. It is initiated by the DNA damage-sensing kinases ATM and ATR, which activate downstream kinases CHEK1 and CHEK2. *PPM1D* (also known as WIP1) acts as a negative regulator by dephosphorylating key DDR components, including *TP53*,

CHEK1, and CHEK2, thereby terminating the DDR signal [15, 16]. This cascade coordinates cell cycle arrest, DNA repair, and apoptosis. Loss-of-function mutations in DDR genes are linked to human syndromes characterized by genomic instability and cancer predisposition—for example, *ATM* and *TP53* mutations underlie ataxia telangiectasia and Li-Fraumeni syndrome, respectively [17]. *CHEK2* mutations are similarly associated with familial cancer predisposition syndromes [18–20]. In line with this, *Chek2*-deficient mice exhibit radioresistance but are more susceptible to genotoxic stress-induced skin cancers [21–24]. More recently, germline *CHEK2* mutations have been linked to CH, particularly in association with the acquisition of somatic *DNMT3A* (but not biallelic *CHEK2* loss) mutations [25]. These findings support a role for CHEK2 in restraining cellular proliferation following DNA damage. However, whether CHEK2 functions within hematopoietic stem/progenitor cells (HSPCs) to confer resistance to genotoxic stress in vivo remains unclear.

Using a genome-wide CRISPR/Cas9 screen, we found that loss of *CHEK2* confers resistance to cytotoxic chemotherapy in hematopoietic cells. *Chek2*-deficient HSPCs were positively selected following chemotherapy treatment in vivo, mimicking the dynamics of t-CH. These cells persisted despite accumulating elevated levels of DNA damage, consistent with the role of CHEK2 in activating the DNA damage checkpoint. Furthermore, we discovered that DNA hypomethylating agents—commonly used frontline therapies for hematologic malignancies—also select for *Chek2*-deficient HSPCs. This selection appears to be driven by DNA damage resulting from the formation of toxic DNA-protein conjugates, rather than by DNA hypomethylation.

¹Graduate Program in Development, Disease Models & Therapeutics, Baylor College of Medicine, Houston, TX, USA. ²Department of Molecular and Human Genetics, Baylor College of Medicine, Houston, TX, USA. ³Division of Biology and Biomedical Sciences, Washington University in St. Louis, St. Louis, MO, USA. ⁴Department of Anesthesiology, Critical Care and Pain Medicine, McGovern Medical School, University of Texas Health Science Center at Houston, Houston, TX, USA. ⁵Division of Pediatric Hematology/Oncology, Department of Pediatrics, Pennsylvania State University College of Medicine, Hershey, PA, USA. ✉email: nakada@bcm.edu

Received: 8 July 2025 Revised: 19 November 2025 Accepted: 12 December 2025
Published online: 12 January 2026

METHODS

Animals

All procedures were approved by Baylor College of Medicine (BCM) Institutional Animal Care and Use Committees (protocol #AN-5858). *Chek2*^{fl/fl} (C57BL/6N-A^{tm1Brd}) *Chek2*^{tm1a(EUCOMM)Hmgu} (JMMuCD) was obtained from MMRRC. *Mx1-Cre* (B6.Cg-Tg^{(Mx1-cre)1Cgn}/J, JAX:003556), CD45.1 (B6.SJL-Ptprc^a Pepc^b/BoyJ, JAX: 002014), and C57BL/6 mice (C57BL/6 J, JAX: 000664) were from JAX. Cisplatin was dissolved in 0.9% NaCl for intraperitoneal injection. Mice were not randomized nor excluded. Investigators were not blinded. Sample sizes were chosen based on observed effect sizes and standard errors from previous experiments.

Cell lines and cell culture

MOLM-13 cells (authenticated by Cytogenetic and Cell Authentication Core at the University of Texas MD Anderson Cancer Center) were cultured in RPMI-1640 with 10% FBS and 1% Penicillin-Streptomycin (ThermoFisher Scientific). HEK293T cells were cultured in DMEM with 10% FBS and 1% Penicillin-Streptomycin. Mouse lineage⁻c-kit⁺Sca-1⁺ (LSK) cells were sorted and cultured in X-Vivo 15 (#04-418Q, Lonza) supplemented with 50 ng/ml SCF, 50 ng/ml TPO, 10 ng/ml IL-3, and 10 ng/ml IL-6 (all from Peprotech). For competitive culture assays, sgRNA/BFP⁺-transduced cells were sorted and mixed with BFP⁻ cells and treated with cisplatin (0.6 μ M), azacitidine (0.5 μ M), decitabine (0.1 μ M), or DMSO. Gene editing with Cas9-sgRNA RNP complex was performed as previously described [26].

Whole genome CRISPR knockout screening

Whole genome CRISPR knockout screening was performed as previously described, with minor modifications [27]. Cas9-expressing MOLM-13 cells, generated by transducing MOLM-13 cells with a lentiviral Cas9 vector (pKLV2 EF1aBsd2ACas9-W, Addgene # 68343), were transduced with a lentiviral whole-genome sgRNA library (Addgene #67989) at a multiplicity of infection of 0.3. Cells were then treated with 0.5 μ M cisplatin, 0.6 μ M melphalan, or DMSO, and cultured for 25 days. On day 25, 10^8 were harvested for genomic DNA (gDNA) preparation, PCR amplification, library preparation, and data analysis as before [27].

Competitive bone marrow transplantation

5 \times 10⁵ experimental bone marrow cells (CD45.2⁺) were mixed with 2 \times 10⁶ competitor bone marrow cells (CD45.1⁺) and transplanted into lethally irradiated (two doses of 500 cGy) CD45.1⁺ recipient mice via tail vein injection. Peripheral blood was collected from recipient mice at the indicated time point after transplantation, and donor chimerism was assessed in Mac-1⁺Gr-1⁺ myeloid cells, B220⁺ B-cells, and CD3⁺ T-cells within CD45.1⁺ and CD45.2⁺ cells by flow cytometry.

Flow cytometry and HSPC isolation

Extraction of bone marrow cells and isolation of HSPCs, including immunofluorescence staining of HSPCs, were done as previously described [28]. Hematopoietic progenitor populations analyzed include hematopoietic stem cells (HSCs, CD150⁺CD48^{-/low}lineage⁻Sca-1⁺c-kit⁺(LSK)), multipotent progenitor populations (CD150⁺CD48^{-/low}LSK), HPC1 (CD150⁺CD48⁺LSK), HPC2 (CD150⁺CD48⁺LSK), granulocyte-macrophage progenitors (GMPs, lineage⁻Sca-1⁺c-kit⁺ CD34⁺CD16/32⁺), megakaryocyte erythroid progenitors (MEPs, lineage⁻Sca-1⁺c-kit⁺ CD34⁺CD16/32⁺), and common myeloid progenitors (CMPs, lineage⁻Sca-1⁺c-kit⁺ CD34⁺CD16/32⁺). BrdU incorporation was assessed using the APC BrdU kit (BD Biosciences, #552598) according to the manufacturer's instructions. Apoptosis was assessed using the Annexin V-APC Apoptosis Detection Kit I (BD Pharmingen, #550475) following the manufacturer's instructions. Nonviable DAPI⁺ cells were excluded from sorts and analyses. Unless otherwise noted, antibodies were obtained from BioLegend, BD Biosciences, or eBioscience. Flow cytometry was performed with LSR II, LSRFortessa, or FACSSymphony flow cytometers (BD Biosciences).

Drug screening

The Approved Oncology Drugs Set X (plates 4893-4895) was obtained from the National Cancer Institute. A 1:1 mixture of BFP⁻ *CHEK2* WT and BFP⁺ *CHEK2* KO cells was plated into 96-well plates at 10000 cells/well and exposed to the drugs diluted to 200 or 500 nM with RPMI-1640 along with DMSO as a control. After 3-4 days of drug treatment, cells were analyzed by flow cytometry. Drugs that were selected for or against *CHEK2*-mutant cells were identified by z-score ranking. Drugs with a z-score greater than 2

were used to profile the enriched drug category, positively selecting *CHEK2* mutations.

Statistical analysis

Statistical analyses were performed by one-way ANOVA, unpaired two-tailed Student's *t*-test, or multiple *t*-tests using GraphPad Prism 8.0.2 (GraphPad Software). A *p*-value of 0.05 or lower was considered significant. Animal studies were performed without blinding.

RESULTS

CHEK2 loss confers chemotherapy resistance

To identify genes that confer chemotherapy resistance to hematopoietic cells, we performed a whole-genome CRISPR knock out (KO) screen with MOLM-13 AML cells expressing Cas9 (Fig. 1A). We transduced cells with a human genome-wide CRISPR library consisting of 90,709 single guide RNAs (sgRNAs) targeting 18,010 genes [29] and treated them with cisplatin, melphalan, or DMSO control. The cells were harvested after 15–20 cell doublings, and the sgRNA representation was analyzed by MAGeck [30]. By comparing the sgRNA abundance with or without chemotherapies, we identified 763 and 1,479 genes significantly enriched following cisplatin or melphalan treatment, respectively. These positively selected genes were enriched for biological processes such as responses to stimuli and stresses, telomerase and cellular aging, and regulation of cell cycle progression (Supplementary Fig. 1A–D, Supplementary Table 1). In particular, *CHEK2* was among the most significantly dropped out genes following both treatments (Fig. 1B, C). *CHEK2* encodes checkpoint kinase 2 (CHK2), a key regulator of the DNA damage response (DDR) involved in cell cycle activation, apoptosis, and DNA repair. This finding aligns with previous studies demonstrating that hematopoietic clones carrying mutations in DDR genes, such as *PPM1D*, *TP53*, and *CHEK2*, are positively selected after exposure to chemotherapies [9–12].

To determine how *CHEK2* mutations affect chemosensitivity, we deleted *CHEK2* from MOLM-13 AML cells by using two methods: a lentiviral CRISPR-Cas9 system to generate *CHEK2* KO cells that can be tracked by BFP or by a Cas9-sgRNA ribonucleoprotein complex strategy to create clonal *CHEK2* KO cells after single-cell cloning (Supplementary Figs. 1E–G). Cisplatin treatment activated the DDR in a dose-dependent manner, as indicated by increased phospho-CHEK2 Thr68 and phospho-p53 Ser15 (Fig. 1D and Supplementary Fig. 1M), key signal transducers in response to DNA damage. Consistent with the role of *CHEK2* in activating p53, phosphorylation of p53 at Ser15 was reduced in *CHEK2* KO cells. *CHEK2* deletion significantly enhanced resistance to cisplatin, melphalan, and bleomycin (Supplementary Figs. 1H–J), suggesting that blunted DDR may confer resistance to chemotherapies.

To better understand how *CHEK2* mutation affects the fitness of cells upon chemotherapy exposure, we performed in vitro competitive assays. We mixed blue fluorescent protein (BFP)⁻ *CHEK2* wild-type (WT) and BFP⁺ *CHEK2* KO cells at a 7:3 ratio and treated them with cisplatin or control DMSO. *CHEK2* KO cells exhibited no growth advantage without chemotherapies. However, *CHEK2* KO cells outcompeted their WT counterparts following cisplatin treatment, leading to the expansion from 28.5% to 86.4% over 17 days (Fig. 1E, F). Similarly, deletion of *TP53* alone or together with *CHEK2* also conferred competitive growth advantage in the presence of cisplatin (Supplementary Figs. 1K, L). The expansion of *CHEK2* mutant cells correlated with dysregulated DNA damage responses. In contrast to WT cells that exhibited G2/M-arrest and apoptosis, *CHEK2* KO cells maintained cell cycle progression as evidenced by a higher frequency of cells in S-phase and the expansion of cell numbers under cisplatin treatment compared to WT cells (Fig. 1G–I). Apoptosis was notably suppressed in *CHEK2* KO cells, indicated by a reduced proportion of PI⁻/Annexin V⁺ cells compared to WT cells (Fig. 1J) and lower protein levels of cleaved caspase-3 (Fig. 1D and Supplementary Fig. 1N). These findings

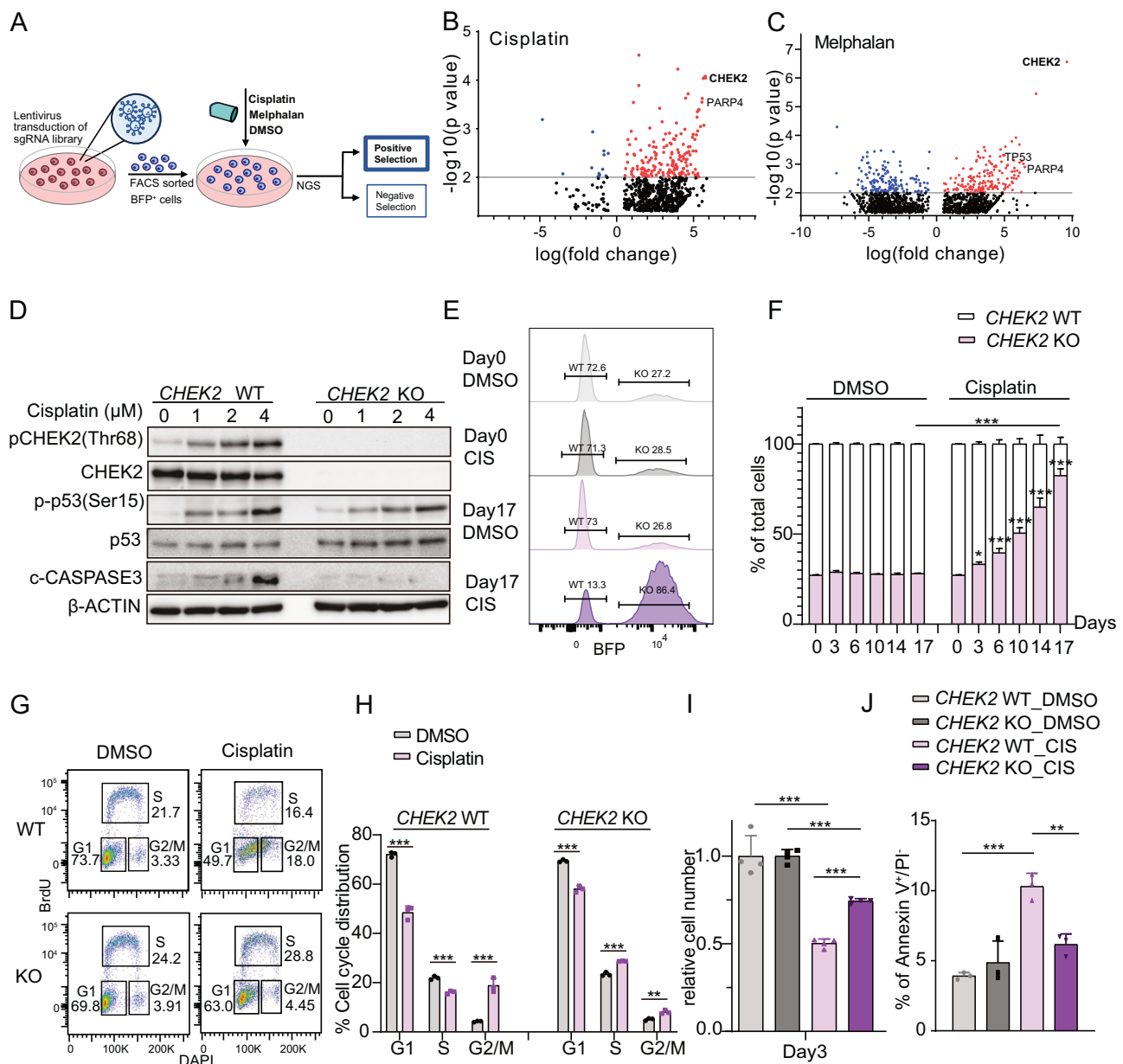


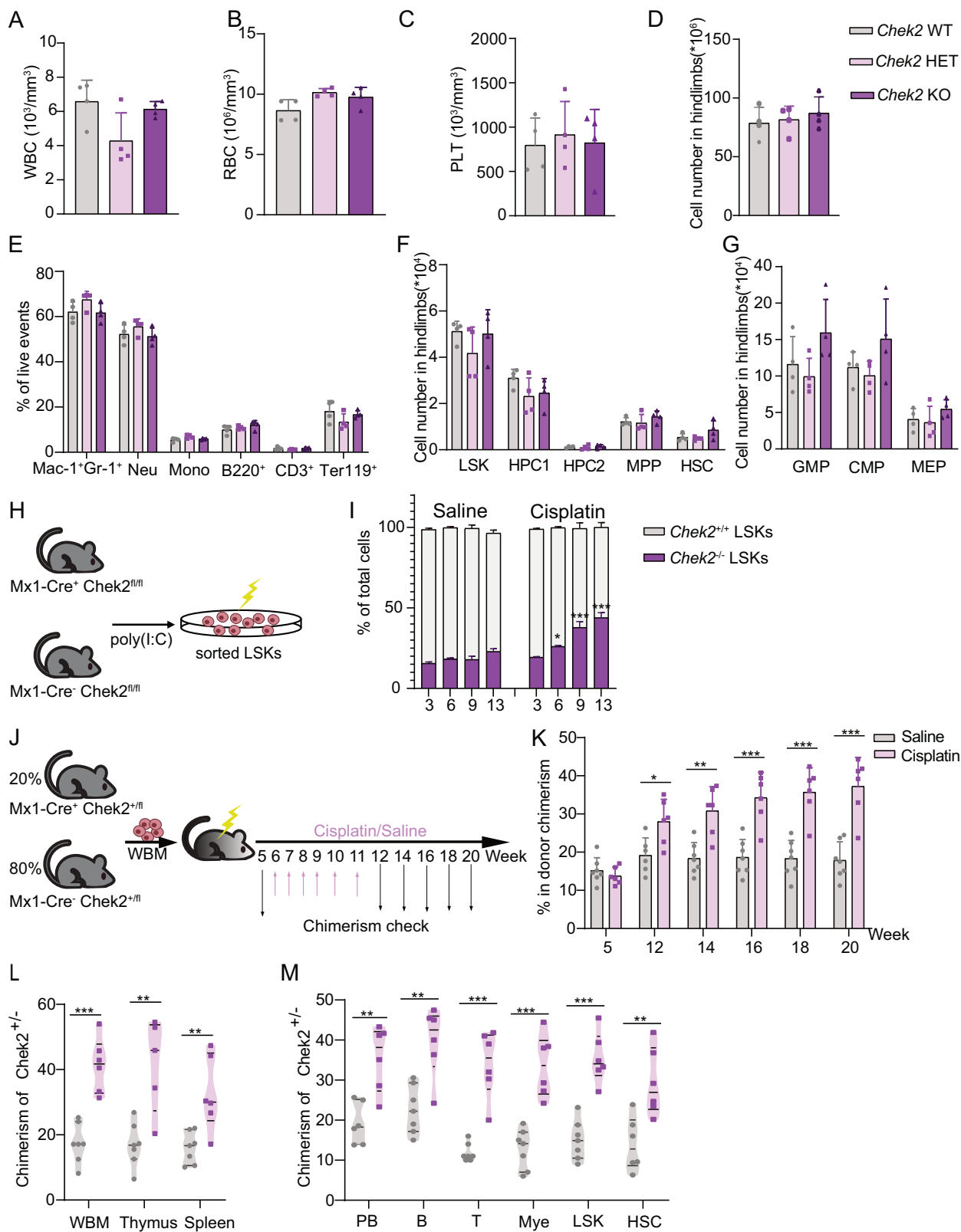
Fig. 1 *CHEK2* loss confers resistance to genotoxic stressors. **A** Schematic representation depicting the CRISPR screening approach to identify genes that confer chemoresistance to AML cells. Volcano plots showing the genes that were enriched or dropped out upon cisplatin (**B**) or melphalan (**C**) treatment. Genes with $\log(\text{fold change}) > 0.5$ or < -0.5 with $p\text{-value} < 0.05$ are displayed. **D** Immunoblot analysis of *CHEK2* wild type (WT) and knock out (KO) AML cells treated with the indicated doses of cisplatin. Representative histograms (**E**) and quantification (**F**) of competitive cell culture assays with *CHEK2* WT and KO cells with or without cisplatin treatment ($n = 3$). Representative flow cytometry plots (**G**) and quantification (**H**) of cell cycle distribution in *CHEK2* WT and KO cells with or without cisplatin treatment ($n = 3$). The effects of cisplatin on cell expansion (**I**), and apoptosis (**J**) of *CHEK2* WT and KO cells ($n = 4$ for **I**; and $n = 3$ for **J**). All data are represented as mean \pm standard deviation (SD). * $p < 0.05$; ** $p < 0.01$; and *** $p < 0.001$. p values were calculated by one-way ANOVA with Sidak's multiple comparison analysis (**F**, **I**, and **J**), multiple t-test with Holm-Sidak correction (alpha = 0.05) (**H**). See also Supplementary Fig. 1.

suggest that the attenuated DDR caused by *CHEK2* deletion confers resistance to genotoxic chemotherapies.

Chek2 deficiency provides a selective advantage under cisplatin treatment

To investigate how *Chek2* loss affects the hematopoietic system following exposure to genotoxic chemotherapies, we generated a *Chek2* conditional KO model by crossing *Chek2^{f/f}* with *Mx1-Cre* mice. *Mx1-Cre; Chek2^{f/f}*, *Mx1-Cre; Chek2^{+/f}*, and control *Mx1-Cre; Chek2^{+/+}* mice were treated with polyinosinic:polycytidyl acid (poly(I:C)) to induce Cre (hereafter referred to as *Chek2* KO, HET,

and WT; Supplementary Figs. 2A–C). We found that *Chek2* homozygous or heterozygous deletion had no impact on peripheral blood cell counts, bone marrow cellularity, the composition of cells in the bone marrow, or the numbers of bone marrow hematopoietic stem and progenitor cells (HSPCs; Fig. 2A–F; Supplementary Fig. 2D–H). Specifically, we found no differences in the number of lineage⁻Sca-1⁺c-kit⁺ (LSK) cells, CD150⁺CD48⁻LSK HSCs, common myeloid progenitors (CMP), granulocyte-monocyte progenitors (GMP), and megakaryocyte-erythroid progenitors (MEP) in the bone marrow (Fig. 2F, G). Thus, *Chek2* function is dispensable for steady-state hematopoiesis.



To begin to determine whether Chek2-deficient HSPCs gain competitive advantage upon genotoxic stresses, we performed competitive culture assays in which we co-cultured Chek2 WT and KO LSK cells and exposed them to cisplatin. Similarly to CHEK2-deficient AML cell lines, Chek2-deficient LSK cells outcompeted WT

LSK cells only when they were exposed to cisplatin (Fig. 2H, I). We then examined the fitness advantage of Chek2 mutant cells in vivo by competitive bone marrow transplantation assays. We transplanted a mixture of 20% CD45.2⁺ Chek2 HET cells and 80% CD45.1⁺ Chek2 WT cells, and the CD45.2:CD45.1 ratio was

Fig. 2 *Chek2* mutant HSPCs outcompete WT cells upon cisplatin treatment. Cell counts of white blood cells (WBC, **A**), red blood cells (RBC, **B**), and platelets (PLT, **C**) of *Chek2* WT, HET and KO mice ($n = 4$ per group). **D** Bone marrow cellularity of *Chek2* WT, HET, and KO mice from two hindlimbs ($n = 4$ per group). **E** The frequencies of the indicated cell population in the bone marrow ($n = 4$ per group). The absolute cell number of the indicated immature hematopoietic stem/progenitor cell populations (**F**) and myeloid progenitor populations (**G**) in mice as in **(A–E)**. A schematic representation of competitive culture assays (**H**) and quantification (**I**) performed with *Chek2* WT or KO LSK cells treated with or without cisplatin ($n = 3$ per group). **J** A schematic representation of the competitive bone marrow transplantation assay with *Chek2* WT and HET whole bone marrow (WBM) cells. Mice were treated with weekly cisplatin or saline treatment for 6 consecutive weeks from week 6–12 after transplantation. **K** The overall peripheral blood chimerism from *Mx1-Cre; Chek2^{+/fl}* (*Chek2* HET) cells in recipient mice treated with saline or cisplatin ($n = 7$ for saline-treated group; and $n = 6$ for cisplatin treated group). Terminal analysis of recipient mice shown in **(K)** at 21 weeks post-transplantation. Donor type chimerism from *Chek2* HET cells in whole bone marrow WBM, thymus, and spleen (**L**), as well as peripheral blood (PB, **B**–, T-, myeloid (Mye) cells, LSK, and HSC (**M**) are shown. All data are represented as mean \pm SD. p values in this figure were calculated by one-way ANOVA with Sidak's multiple comparison analysis (**I**), and multiple t-test with Holm-Sidak correction ($\alpha=0.05$) (**K–M**). See also Supplementary Fig. 2.

monitored over time before and after cisplatin treatment (Fig. 2J). We studied the effects of *Chek2* heterozygosity since it better models human CHIP than homozygous deletion. *Chek2* heterozygosity did not affect the reconstitution levels of mice treated with control saline, consistent with our observation that *Chek2* loss does not affect steady-state hematopoiesis. On the contrary, *Chek2* HET cells significantly outcompeted WT cells upon cisplatin treatment, increasing their overall chimerism from an average of 13.8% (range of 11.1–17.0%) at 5 weeks to 35.5% (range of 23.3–43.3%) at 20 weeks (Fig. 2K). *Chek2* HET cells in all three hematopoietic lineages (myeloid, T-, and B-cell lineages) and all major hematopoietic organs analyzed (bone marrow, thymus, spleen) showed enhanced fitness after cisplatin treatment (Fig. 2K, L, and Supplementary Figs. 2I–K). This fitness advantage could be traced back to the top of the hematopoietic hierarchy, since *Chek2* heterozygous HSCs and LSK cells outcompeted WT cells upon cisplatin treatment (Fig. 2M). Together, these data indicate that *Chek2* mutations confer a selective advantage to HSCs and hematopoiesis when exposed to genotoxic stressors.

Chek2-deficient HSPCs are spared from genotoxic stressor exposure

To explore the mechanism underlying the clonal expansion of *Chek2* mutant cells, we compared the responses of *Chek2* WT and KO hematopoietic cells to cisplatin treatment. We treated *Chek2* WT and KO mice with four daily injections of cisplatin and analyzed the hematopoietic compartment four days after the last injection (day 8) (Fig. 3A). Both *Chek2* WT and KO mice exhibited reduced bone marrow cellularity (Fig. 3B), white blood cell, red blood cell, and platelet counts with no differences between the two genotypes (Fig. 3C–E, and Supplementary Figs. 3A–C). While cisplatin treatment did not alter the lineage distribution in peripheral blood (Supplementary Fig. 3D), it led to an increased frequency of myeloid cells and a reduction in B- and erythroid cells in the bone marrow (Fig. 3F). *Chek2* deletion partially mitigated these changes.

In contrast to these modest differences between WT and *Chek2* KO hematopoiesis upon cisplatin treatment, WT and *Chek2* KO HSPCs exhibited significant differences in response to cisplatin. Continuous exposure to cisplatin resulted in substantial depletion of immature HSPCs, including LSK, CD150⁺CD48⁺LSK hematopoietic progenitor cell 1 (HPC1), multipotent progenitors (MPPs), and HSCs (Fig. 3G, and Supplementary Fig. 3E). Myeloid progenitors CMPs, GMPs, and MEPs were also reduced by cisplatin treatment (Fig. 3H, and Supplementary Fig. 3F). The depletion of these HSPC populations was significantly ameliorated by *Chek2* deficiency. Collectively, these results establish that *Chek2* loss confers chemotherapy resistance to HSPCs.

Chek2-deficient HSCs persist with increased DNA damage after genotoxic stressors

Previous studies have suggested that HSPCs harboring mutations in DDR genes, such as *PPM1D*, *TP53*, and *SRCP*, display altered levels of DNA damage when exposed to cytotoxic chemotherapy

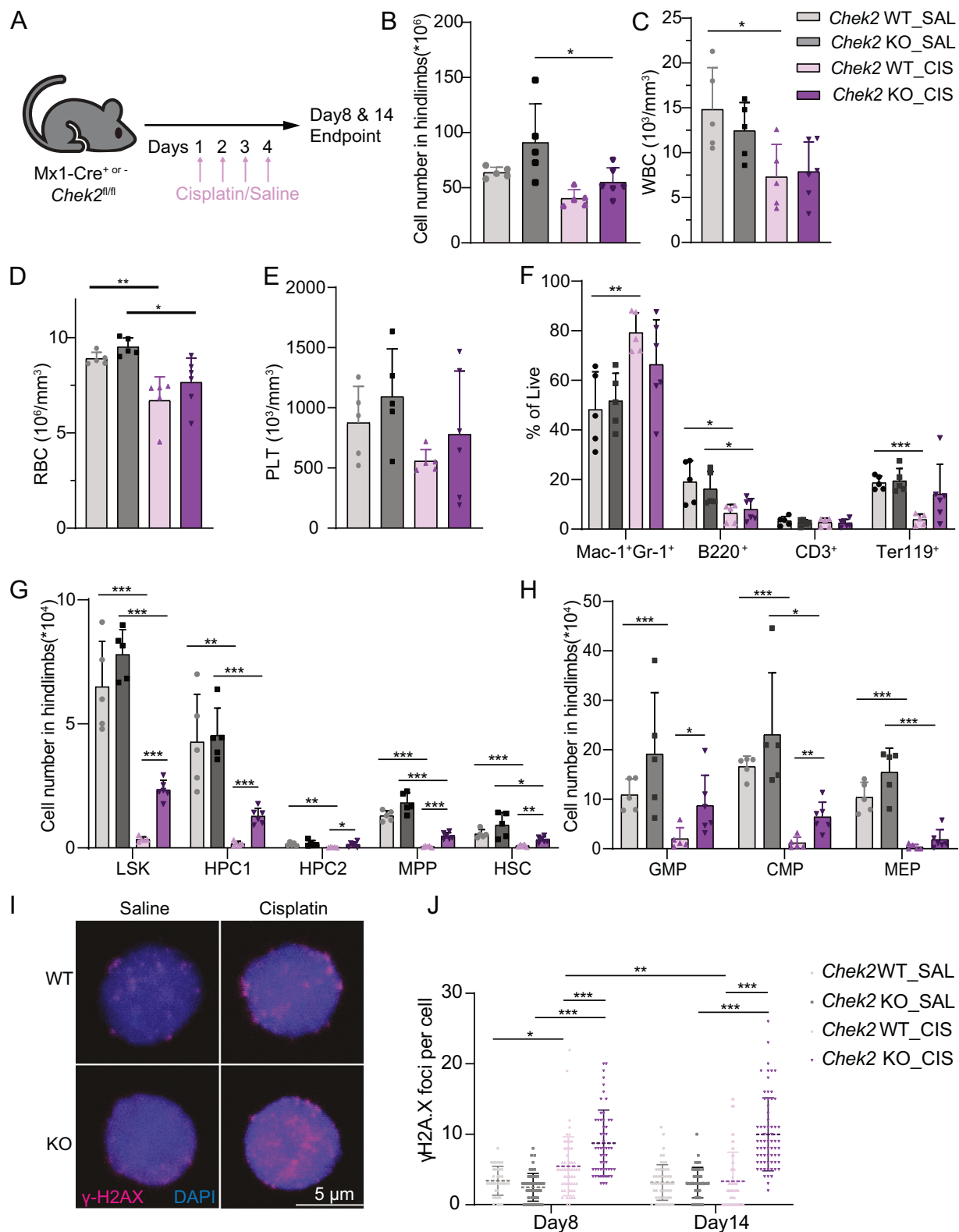
[31–33]. *Chek2* WT and KO LSK cells displayed comparable γ H2AX levels, an indicator of DNA double-strand breaks (DSBs), in saline-treated controls. Four days after four daily cisplatin exposure (as in Fig. 3), γ H2AX levels in *Chek2* WT LSKs were significantly increased compared to those treated with saline (Fig. 3I), consistent with the finding that cisplatin significantly depleted HSPCs in WT mice (Fig. 3G). Notably, *Chek2*-mutant LSKs exhibited higher levels of γ H2AX foci formation than WT LSKs after cisplatin treatment (Fig. 3I, J).

To capture DNA damage levels in HSPCs when the hematopoietic system recovers from cisplatin treatment, we analyzed the mice ten days after four daily cisplatin treatment (day 14). At this time point, bone marrow cellularity, white blood cell, red blood cell, and platelet counts largely recovered and showed no difference between the two genotypes or with saline-treated control mice (Supplementary Fig. 3H–K). The frequencies of mature hematopoietic cells in the peripheral blood and bone marrow were also indistinguishable between cisplatin- and saline-treated mice (Supplementary Figs. 3L, M).

In contrast to mature hematopoietic cells, HSPCs exhibited delayed recovery following cisplatin treatment. While both *Chek2* WT and KO HSPC populations such as LSK, HPC1, MPP, GMP, and CMP were significantly reduced at day 14 of cisplatin treatment compared to saline-treated mice, *Chek2* KO mice exhibited accelerated recovery compared to *Chek2* WT mice (Supplementary Figs. 3N, O). By day 14, DNA damage (as assessed by the numbers of γ H2AX foci) had largely resolved in *Chek2* WT LSK cells. In contrast, *Chek2* KO LSK cells retained high levels of γ H2AX foci, similar to those observed on day 8, with no significant change between days 8 and 14 (Fig. 3J and Supplementary Fig. 3P). Colony-forming assays revealed that *Chek2* WT HSCs had slightly reduced colony-forming capacity in semi-solid medium, suggesting that cisplatin-induced DNA damage modestly impaired HSC function. *Chek2* KO HSCs exhibited a similar reduction in colony-forming capacity (Supplementary Fig. 3G). These findings suggest that *Chek2* KO HSCs retain the ability to repair DNA damage, potentially upon exiting quiescence and entering the cell cycle, as previously reported [34]. Combined with the observation that *Chek2*-deficient cells undergo attenuated cell cycle arrest and apoptosis following DNA damage (Fig. 1), these results indicate that *Chek2* deficiency enables HSPCs to persist despite sustained DNA damage.

CHEK2 deficiency confers resistance to hypomethylating agents

Previous studies with solid tumor cell lines and models have shown that *CHEK2* KO cells exhibit resistance to a wide spectrum of DNA-damaging agents. This raised the possibility that *CHEK2* loss may confer chemoresistance to hematopoietic cells against a broader spectrum of chemotherapies than currently known, including those that are used to treat hematologic malignancies. To address this question, we performed a drug screening to identify therapies that select *CHEK2* mutant hematopoietic cells.



We mixed *CHEK2* WT (BFP⁺) and KO (BFP⁺) MOLM-13 cells at a 1:1 ratio and exposed them to a panel of FDA-approved cancer chemotherapies (Fig. 4A). As expected, we found that cytotoxic chemotherapies such as melphalan, doxorubicin, etoposide, and bleomycin positively selected *CHEK2* mutant cells (Supplementary

Table 2). Interestingly, top hits that selected for *CHEK2*-mutant cells included two hypomethylating agents (HMAs): azacitidine (AZA) and decitabine (DAC) (Fig. 4A, B). Given that HMAs are frontline therapies to treat hematologic malignancies, including myelodysplastic syndrome (MDS), myeloproliferative neoplasm

Fig. 3 *Chek2*-deficient are resistant to cisplatin treatment. **A** An experimental scheme to analyze the effects of cisplatin treatment on hematopoiesis. **B** Bone marrow cellularity of *Chek2* WT and KO mice treated with or without cisplatin ($n=5$ per group, except $n=6$ for cisplatin-treated *Chek2* KO mice). Cell counts of white blood cells (WBC, **C**), red blood cells (RBC, **D**), and platelets (PLT, **E**) of mice as in **(B)**. **F** The frequencies of the indicated cell population in the bone marrow of *Chek2* WT or KO mice treated with or without cisplatin. The absolute numbers of the indicated immature hematopoietic stem/progenitor cell populations (**G**) and myeloid progenitor populations (**H**) in mice as in **(B–F)**. Representative immunofluorescence images (**I**) and quantification of the numbers of γ H2AX foci per cell (**J**) in LSK cells isolated from *Chek2* WT or KO mice treated with or without cisplatin at day 8 and day 14. Scale bar, 5 μ m. All data are represented as mean \pm SD. *p*-values in this figure were calculated by one-way ANOVA with Sidak's multiple comparison analysis (**B–D**, and **J**), multiple t-test with Holm-Sidak correction ($\alpha=0.05$) (**F–H**). See also Supplementary Fig. 3.

(MPN), and AML, we focused on understanding the mechanisms driving HMA resistance in *CHEK2* KO cells. We validated the effects of HMA by conducting competitive culture assays in which BFP⁺ *CHEK2* KO cells are mixed with BFP⁺ *CHEK2* WT at a starting ratio of 3:7 and treated with HMAs. *CHEK2*-mutant cells did not show any growth advantage when treated with vehicle control, but they outcompeted *CHEK2* WT cells upon exposure to AZA or DAC treatment (Fig. 4C). Consistently, the cytotoxic/cytostatic effects of AZA and DAC were mitigated by *CHEK2* mutations (Fig. 4D, Supplementary Figs. 4A, B).

To test whether *CHEK2* loss confers selective advantage to HSPCs when exposed to HMAs, we conducted an *ex vivo* competitive culture assay with 80% *Chek2* WT (CD45.1⁺) and 20% *Chek2* KO (CD45.2⁺) LSK cells (Fig. 4E). Similarly to the results obtained with AML cells, *Chek2* KO LSK cells outcompeted WT cells when exposed to HMAs but not to vehicle (Fig. 4F). Thus, HMAs, similarly to genotoxic stressors such as cisplatin and melphalan, select for *CHEK2*-mutant cells, including immature HSPCs.

To better understand how *CHEK2* mutations confer a selective advantage under HMA exposure, we examined apoptosis and proliferation. AZA and DAC increased apoptotic cells and reduced cells in the S-phase; both of these changes were mitigated by *CHEK2* deletion (Fig. 4G, H), consistent with the finding that *CHEK2* KO cells expanded more than WT cells when exposed to AZA or DAC (Fig. 4D). These results suggest that the resistance of *CHEK2* mutant cells to HMAs is associated with defective cell cycle arrest and reduced apoptosis.

CHEK2 mutations in blood are enriched in cancer patients receiving genotoxic chemotherapies such as platinum agents or topoisomerase inhibitors, but it has not been shown whether *CHEK2*-mutant hematopoietic cells expand in individuals treated with HMA, or whether *CHEK2* expression affects HMA sensitivity. To begin to gain insights into this question, we analyzed a published RNA-seq dataset of myelodysplastic syndromes/chronic myelomonocytic leukemia (MDS/CML) patients treated with AZA [35]. As shown previously [35], DDR-related pathways such as G2/M DNA damage checkpoint signaling, G1/S checkpoint regulation, and ATM signaling, were activated in AZA responding patients. To begin to understand the role of the DDR pathway in HMA sensitivity, we took the intersection of 3288 differentially expressed genes (DEG) between AZA non-responders and responders and 975 DDR-related genes from UniProtKB, resulting in 220 genes. To determine whether these 220 DDR genes differentially expressed between AZA non-responders and responders are enriched for *CHEK2* substrates, we analyzed a published serine/threonine kinase substrate profiling study [36]. We found that these 220 genes were significantly more enriched in *CHEK2* substrates than the remaining 775 DDR genes that were not differentially expressed between AZA non-responders and responders (61 out of 220 vs. 157 out of 775, odds ratio = 1.46, $p=0.0375$; Fig. 4I, Supplementary Fig. 4C, and Supplementary Table 3). The *CHEK2* substrates that were differentially expressed between AZA responding vs. non-responding patients include CDC25A, CDC25C, CDK1, and CDK2, which are known to regulate cell cycle progression as well as MDM2, an established p53 regulator involved in apoptosis (Supplementary Fig. 4C and

Supplementary Table 3). Collectively, these findings suggested that HMA treatment triggers the DDR in myeloid malignancies, partly through *CHEK2* which triggers cell cycle arrest and apoptosis, and that the failure to mount the DDR is associated with HMA resistance.

AZA and DAC are metabolized to 2'-deoxy-5-azacytidine-triphosphate (5-aza-dCTP), which is incorporated into DNA during replication and covalently traps DNA methyltransferases, primarily DNMT1, on the DNA. This depletes DNMT1, leading to hypomethylation of DNA. It also produces DNMT1-DNA covalent adducts, a form of highly toxic DNA damage [37] (Fig. 5A). On the contrary, a non-covalent DNMT1 inhibitor GSK3484862 competes with the active-site loop of DNMT1 [38]. The two distinct mechanisms by which HMAs and GSK3484862 inhibit DNMT1 provided an opportunity to distinguish the effects of DNA hypomethylation and DNA damage induction in selecting *CHEK2*-mutant cells. To this end, we performed a competitive culture experiment with *CHEK2* WT and KO cells treated with HMA with or without GSK3484862. If DNA hypomethylation selects for *CHEK2*-mutant cells, HMA, GSK3484862, and HMA + GSK3484862 double treatment should all select for *CHEK2*-mutant cells. However, if DNA damage caused by HMA selects for *CHEK2*-mutant cells, the effect of HMA should be mitigated by GSK3484862 because GSK3484862 will prevent the formation of DNMT1-DNA conjugates (Fig. 5A). Consistent with the latter possibility, we found that the ability of HMAs to enrich *Chek2* KO cells was significantly blunted by the addition of GSK3484862, while GSK3484862 alone did not select for *Chek2* KO cells (Fig. 5B, C). Both AZA and DAC activated the DDR as evidenced by increased γ H2AX, phospho-TP53 Ser15, and phospho-CHEK2 Thr68 (Fig. 5D). The observed DDR induction was attenuated by the co-treatment with GSK3484862 (Fig. 5D, E).

To establish whether sensitivity to HMAs depends on DNMT1 protein, we deleted *DNMT1* in both *CHEK2* WT and KO MOLM13 cells with CRISPR and examined the DNA damage response after DAC treatment (Supplementary Figs. 4D, E). DAC treatment induced a DNA damage response as evidenced by elevated levels of phosphorylation at *CHEK2* Thr68, p53 Ser15 and Ser20, and cleaved caspase-3 (Supplementary Fig. 4E). *CHEK2* deletion abolished phospho-CHEK2 and reduced cleaved caspase-3 and p53 phosphorylation levels. Deletion of *DNMT1* largely reduced *CHEK2* and p53 phosphorylation as well as cleaved caspase-3, consistent with the model that HMAs covalently trap DNMT1 to DNA. In a competitive growth assay, *Chek2* KO, *DNMT1* KO, and *Chek2/DNMT1* double KO (dKO) all exhibited a competitive advantage after DAC treatment over wild-type cells (Supplementary Fig. 4F). These results highlight the underappreciated effects of HMA in causing DNA damage through DNMT1 and suggest that *CHEK2*-mutant cells may expand upon HMA treatment *in vivo*.

DISCUSSION

Recent studies have consistently reported an enrichment of DDR mutations in the blood cells of cancer patients. Mutations in DDR genes are widely considered to be a precursor for therapy-related myeloid neoplasms [13]. The expanded clones with DDR

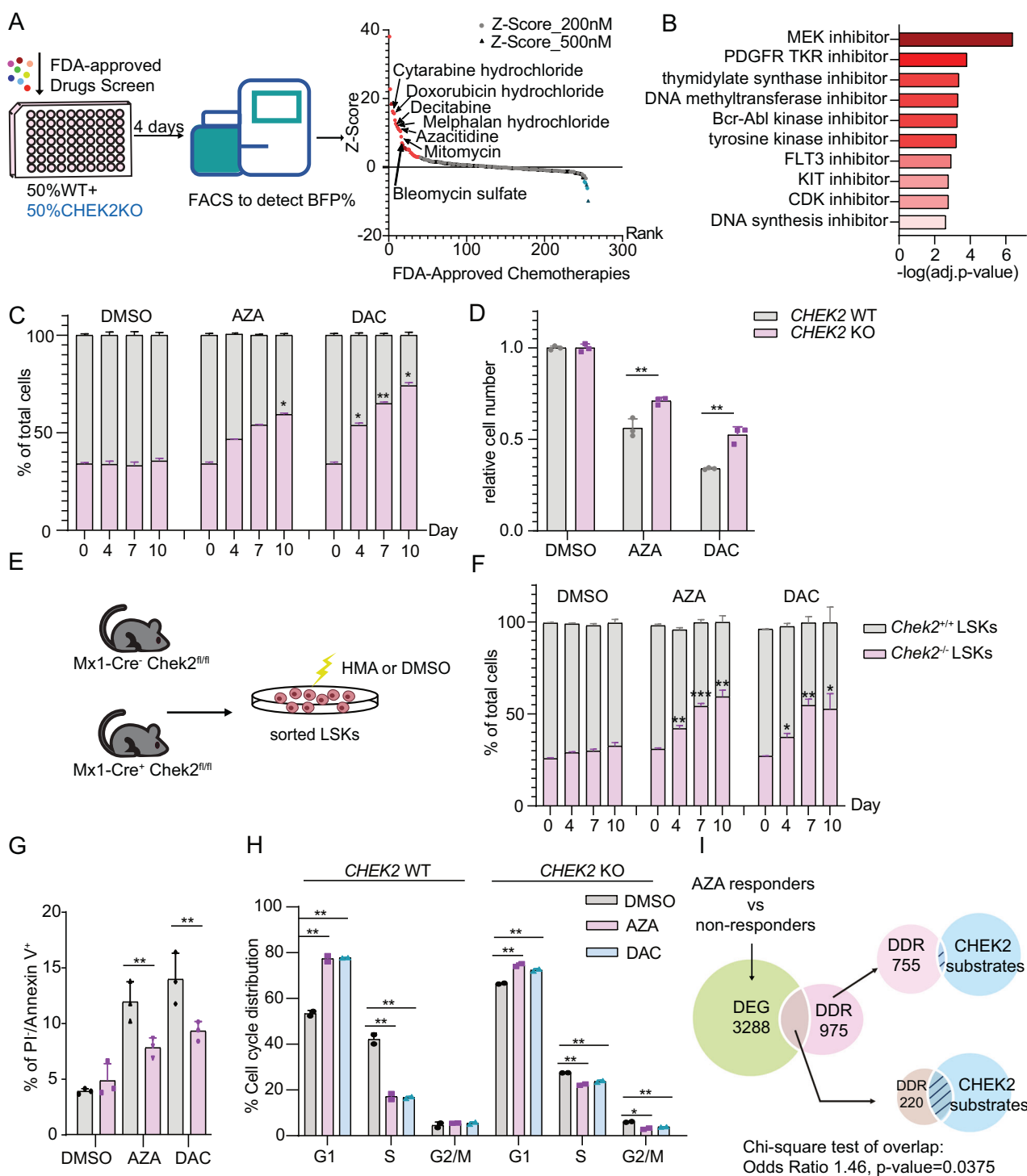


Fig. 4 **CHEK2 loss renders cells resistant to HMA.** **A** An experimental scheme (left) to identify drugs that selects for CHEK2-mutant cells and the waterfall plot showing the z-scores of drugs tested (right). Drug z-scores are plotted against their ranks. **B** Top 10 significantly enriched drug classes ranked by statistical significance identified by the drug screening. **C** Competitive culture assays with CHEK2 WT and KO MOLM-13 cells with or without AZA or DAC treatment ($n = 3$). **D** Relative rates of cell expansion upon AZA or DAC exposure of CHEK2 WT or KO cells at day 2 ($n = 3$). A schematic representation of the competitive culture assays (E) and quantification (F) with Chek2 WT or KO LSK cells treated with or without AZA or DAC ($n = 3$). The effects of AZA or DAC on apoptosis (G), and cell cycle distribution (H) of CHEK2 WT and KO MOLM-13 cells ($n = 2$). **I** A schematic representation of the identification of 220 DDR genes that are differentially expressed between AZA responders and non-responders, and the enrichment of these genes in CHEK2 phosphorylation targets. The 220 DDR genes were significantly enriched for CHEK2 substrates. All data are represented as mean \pm SD. p values in this figure were calculated by log-rank test (B), one-way ANOVA with Sidak's multiple comparison analysis (C, and F), and multiple t-test with Holm-Sidak correction (alpha=0.05) (D, G, and H). See also Supplementary Fig. 4.

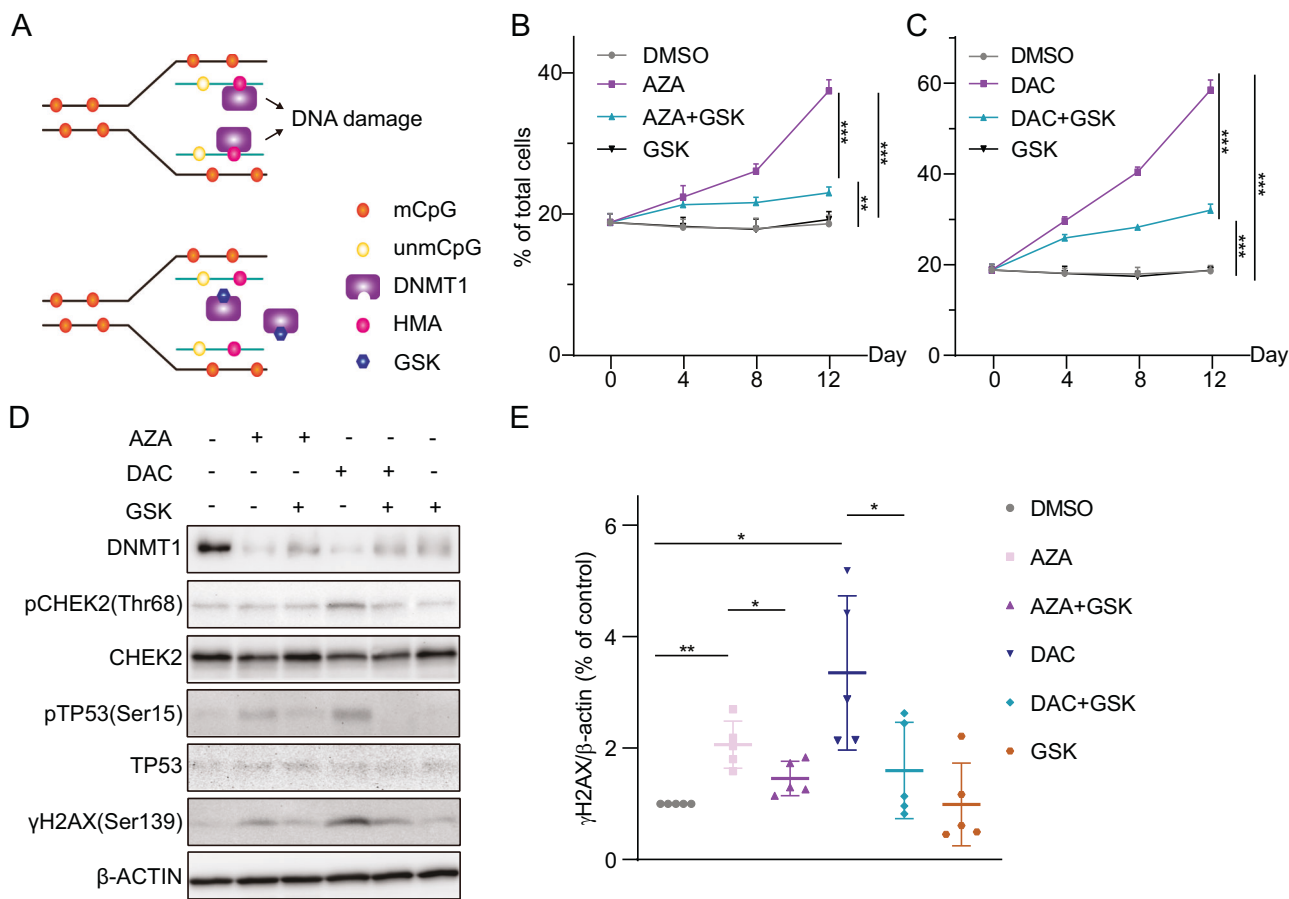


Fig. 5 DNA damage induced by HMA selects for CHEK2-deficient cells. **A** Schematic representation of two distinct mechanisms of action of HMAs and GSK3484862 in causing DNA hypomethylation and DNA damage. HMAs trap DNMT1 by forming DNMT1-DNA conjugates, leading to DNA damage (upper panel). GSK3484862 (GSK) binds to the active site of DNMT1, preventing it from forming the DNMT1-DNA conjugates. **B, C** The frequencies of *CHEK2* KO MOLM-13 cells in competitive culture assays against WT cells with the indicated treatments. The competitive advantage that *CHEK2* KO cells had under HMA exposure was at least partially mitigated by cotreatment with GSK3484862 ($n = 3$). Immunoblot analysis (**D**) and quantification of γ H2AX levels (**E**) of MOLM-13 cells treated with the indicated compounds. The DDR activation observed after AZA or DAC treatment was largely mitigated by GSK3484862 ($n = 5$). All data are represented as mean \pm SD. p -values in this figure were calculated by multiple *t*-test with Holm-Sidak correction ($\alpha=0.05$) (**B** and **C**) or unpaired, two-tailed Student's *t*-test (**E**).

mutations is thought to arise from the chemoresistance conferred by defective DDR pathways: rare cells harboring DDR mutations prior to treatment can evade DNA damage-induced cell cycle arrest or apoptosis, while DDR-proficient cells are eliminated [13]. This selective pressure leads to the expansion of mutant clones. Supporting this hypothesis, murine studies have shown that *Tp53*-mutant HSPCs outcompete WT HSPCs in chimeric mice exposed to genotoxic stress [39, 40].

Similarly, a C-terminal truncation mutation in *Ppm1d*—which results in constitutive phosphatase activity and attenuated DDR—confers hematopoietic cells with both chemoresistance and a competitive advantage over WT cells [11, 12]. Our study demonstrates that loss of *CHEK2*, a recently recognized CH driver [41], also renders hematopoietic cells resistant to genotoxic stress and enables *CHEK2*-mutant cells to outcompete WT counterparts. Under genotoxic stress, immature HSPCs, including HSCs, gain a competitive edge through *Chek2* heterozygosity, explaining the observed dominance of *Chek2*-mutant cells across all three hematopoietic lineages. Similarly, *Chek2* deficiency protects primordial oocytes from chemotherapy-induced attrition [42, 43]. We speculate that this advantage stems from the ability of *Chek2*-mutant cells to evade apoptosis and/or cell cycle arrest. Consistent with this, we show that *Chek2*-mutant HSPCs with elevated DNA damage persist *in vivo*. However, *CHEK2* somatic mutations are rarely found in myeloid malignancies, raising questions regarding

the leukemogenic potential of *CHEK2*-mutant CH clones. Further studies investigating the role of *CHEK2* in leukemogenesis and larger CH cohort studies are needed to delineate the role of *CHEK2* in CH and transformation into myeloid malignancies.

Beyond somatic mutations, germline *CHEK2* mutations also predispose individuals to CH and hematologic malignancies [25, 44–47]. However, the mechanism in this context likely differs: since all cells carry the *CHEK2* mutation in the germline carrier, the selective advantage model does not apply. Instead, germline *CHEK2* loss may facilitate the emergence or persistence of mutant clones by increasing genomic instability or reducing apoptosis and cell cycle arrest. Supporting this hypothesis, AML cases in *CHEK2* germline carriers are enriched for chromosomal translocations involving genes such as *CBFB*, *MECOM*, and *KMT2A* [47]. Germline *CHEK2* variants are also associated with loss of chromosome Y (LOY) [48], a known risk factor for hematologic malignancies [49–51]. We propose that *CHEK2*-deficient HSPCs may act as precursors for these genetic lesions as they can persist with unresolved DNA damage, including double-strand breaks. Thus, our study provides a mechanistic basis for how somatic or germline *CHEK2* deficiency promotes HSPC expansion under genotoxic stress and facilitates further mutagenesis.

We show that *CHEK2*-mutant cells are resistant to HMAs (DAC and AZA) that are widely used to treat hematologic malignancies [52]. Our results indicate that HMAs select for *CHEK2*-mutant cells

through DNA damage rather than DNA hypomethylation. This is supported by the observation that a selective DNMT1 inhibitor, GSK3685032, neither enriched *CHEK2*-mutant cells nor enhanced HMA-driven selection; instead, it attenuated this effect. These findings suggest that other DDR-mutant CH may also be positively selected under HMA exposure. Indeed, *TP53* mutations have been associated with poor outcomes following HMA treatment [53–58], and isogenic *TP53*-mutant AML models confirm that *TP53* loss confers HMA resistance [59]. However, a prospective trial of DAC monotherapy in MDS/AML patients reported favorable responses in *TP53*-mutant cases [60], despite their usual association with poor outcomes under standard cytotoxic chemotherapy. Our results support the former view that DDR mutations confer resistance to HMAs, and the DNA-damaging effects of HMAs—rather than their hypomethylating activity—drive the selection of DDR-mutant clones. Further supporting this notion, we show that DDR pathway and *CHEK2* target genes are reduced in a subset of HMA-nonresponsive myeloid malignancies. Exploiting defective DDR through synthetic lethality—for example, using PARP inhibitors—may provide a targeted therapeutic strategy for HMA-resistant malignancies.

DATA AVAILABILITY

sgRNA sequences and genotyping primers used in this study are listed in Supplementary Table 4. *Chek2*^{fl/fl} mice are available from MMRRC.

REFERENCES

- Genovese G, Kahler AK, Handsaker RE, Lindberg J, Rose SA, Bakhour SF, et al. Clonal hematopoiesis and blood-cancer risk inferred from blood DNA sequence. *N Engl J Med.* 2014;371:2477–87.
- Jaiswal S, Fontanillas P, Flannick J, Manning A, Grauman PV, Mar BG, et al. Age-related clonal hematopoiesis associated with adverse outcomes. *N Engl J Med.* 2014;371:2488–98.
- King KY, Huang Y, Nakada D, Goodell MA. Environmental influences on clonal hematopoiesis. *Exp Hematol.* 2020;83:66–73.
- Hormaechea-Agulla D, Matatall KA, Le DT, Kain B, Long X, Kus P, et al. Chronic infection drives *Dnmt3a*-loss-of-function clonal hematopoiesis via IFNgamma signaling. *Cell stem cell.* 2021;28:1428–42.e6.
- Caiado F, Kovtonyuk LV, Gonullu NG, Fullin J, Boettcher S, Manz MG. Aging drives *Tet2*^{+/−} clonal hematopoiesis via IL-1 signaling. *Blood.* 2023;141:886–903.
- Cai Z, Kotzin JJ, Ramdas B, Chen S, Nelanuthala S, Palani LR, et al. Inhibition of Inflammatory Signaling in *Tet2* Mutant Preleukemic Cells Mitigates Stress-Induced Abnormalities and Clonal Hematopoiesis. *Cell Stem Cell.* 2018;23:833–49.e5.
- Dawoud AAZ, Tapper WJ, Cross NCP. Clonal myelopoiesis in the UK Biobank cohort: *ASXL1* mutations are strongly associated with smoking. *Leukemia.* 2020;34:2660–72.
- Stonestrom AJ, Menghrajani KN, Devlin SM, Franch-Exposito S, Ptashkin RN, Patel SY, et al. High-risk and silent clonal hematopoietic genotypes in patients with nonhematologic cancer. *Blood Adv.* 2024;8:846–56.
- Coombs CC, Zehir A, Devlin SM, Kishtagari A, Syed A, Jonsson P, et al. Therapy-Related Clonal Hematopoiesis in Patients with Non-hematologic Cancers Is Common and Associated with Adverse Clinical Outcomes. *Cell stem cell.* 2017;21:374–82.e4.
- Bolton KL, Ptashkin RN, Gao T, Braunstein L, Devlin SM, Kelly D, et al. Cancer therapy shapes the fitness landscape of clonal hematopoiesis. *Nat Genet.* 2020;52:1219–26.
- Kahn JD, Miller PG, Silver AJ, Sellar RS, Bhatt S, Gibson C, et al. *PPM1D*-truncating mutations confer resistance to chemotherapy and sensitivity to *PPM1D* inhibition in hematopoietic cells. *Blood.* 2018;132:1095–105.
- Hsu JI, Dayaram T, Tovy A, De Braekeleer E, Jeong M, Wang F, et al. *PPM1D* Mutations Drive Clonal Hematopoiesis in Response to Cytotoxic Chemotherapy. *Cell stem cell.* 2018;23:700–13.e6.
- Takahashi N, Nakada D, Goodell M. Distinct landscape and clinical implications of therapy-related clonal hematopoiesis. *J Clin Invest.* 2024;134.
- Jackson SP, Bartek J. The DNA-damage response in human biology and disease. *Nature.* 2009;461:1071–8.
- Lu X, Nannenga B, Donehower LA. *PPM1D* dephosphorylates Chk1 and p53 and abrogates cell cycle checkpoints. *Genes Dev.* 2005;19:1162–74.
- Oliva-Trastoy M, Berthonaud V, Chevalier A, Ducrot C, Marsolier-Kergoat MC, Mann C, et al. The Wip1 phosphatase (*PPM1D*) antagonizes activation of the Chk2 tumour suppressor kinase. *Oncogene.* 2007;26:1449–58.
- Tiwari V, Wilson DM. 3rd. DNA Damage and Associated DNA Repair Defects in Disease and Premature Aging. *Am J Hum Genet.* 2019;105:237–57.
- Bell DW, Varley JM, Szydlo TE, Kang DH, Wahler DC, Shannon KE, et al. Heterozygous germ line *hCHEK2* mutations in Li-Fraumeni syndrome. *Science.* 1999;286:2528–31.
- Cybulski C, Gorski B, Huzarski T, Masojc B, Mierzejewski M, Debnik T, et al. *CHEK2* is a multiorgan cancer susceptibility gene. *Am J Hum Genet.* 2004;75:1131–5.
- Vaheristo P, Bartkova J, Eerola H, Syrjakoski K, Ojala S, Kilpivaara O, et al. A *CHEK2* genetic variant contributing to a substantial fraction of familial breast cancer. *Am J Hum Genet.* 2002;71:432–8.
- Hirao A, Kong YY, Matsuoka S, Wakeham A, Ruland J, Yoshida H, et al. DNA damage-induced activation of p53 by the checkpoint kinase Chk2. *Science.* 2000;287:1824–7.
- Takai H, Naka K, Okada Y, Watanabe M, Harada N, Saito S, et al. Chk2-deficient mice exhibit radioresistance and defective p53-mediated transcription. *EMBO J.* 2002;21:5195–205.
- Hirao A, Cheung A, Duncan G, Girard PM, Elia AJ, Wakeham A, et al. Chk2 is a tumor suppressor that regulates apoptosis in both an ataxia telangiectasia mutated (ATM)-dependent and an ATM-independent manner. *Mol Cell Biol.* 2002;22:6521–32.
- Tanoue Y, Toyoda T, Sun J, Mustafa MK, Tateishi C, Endo S, et al. Differential Roles of Rad18 and Chk2 in Genome Maintenance and Skin Carcinogenesis Following UV Exposure. *J Invest Dermatol.* 2018;138:2550–7.
- Kessler MD, Damask A, O'Keeffe S, Banerjee N, Li D, Watanabe K, et al. Common and rare variant associations with clonal hematopoiesis phenotypes. *Nature.* 2022;612:301–9.
- Gundry MC, Brunetti L, Lin A, Mayle AE, Kitano A, Wagner D, et al. Highly Efficient Genome Editing of Murine and Human Hematopoietic Progenitor Cells by CRISPR/Cas9. *Cell Rep.* 2016;17:1453–61.
- Shi X, Jiang Y, Kitano A, Hu T, Murdaugh RL, Li Y, et al. Nuclear NAD(+) homeostasis governed by NMNAT1 prevents apoptosis of acute myeloid leukemia stem cells. *Sci Adv.* 2021;7.
- Tseng YJ, Kageyama Y, Murdaugh RL, Kitano A, Kim JH, Hoegenauer KA, et al. Increased iron uptake by splenic hematopoietic stem cells promotes TET2-dependent erythroid regeneration. *Nature Commun.* 2024;15:538.
- Tzelepis K, Koike-Yusa H, De Braekeleer E, Li Y, Metzakopian E, Dovey OM, et al. A CRISPR Dropout Screen Identifies Genetic Vulnerabilities and Therapeutic Targets in Acute Myeloid Leukemia. *Cell Rep.* 2016;17:1193–205.
- Li W, Xu H, Xiao T, Cong L, Love MI, Zhang F, et al. MAGeCK enables robust identification of essential genes from genome-scale CRISPR/Cas9 knockout screens. *Genome Biol.* 2014;15:54.
- Chen CW, Zhang L, Dutta R, Niroula A, Miller PG, Gibson CJ, et al. SRCAP mutations drive clonal hematopoiesis through epigenetic and DNA repair dysregulation. *Cell Stem Cell.* 2023;30:1503–19.e8.
- Reinhardt HC, Aslanian AS, Lees JA, Yaffe MB. p53-deficient cells rely on ATM- and ATR-mediated checkpoint signaling through the p38MAPK/MK2 pathway for survival after DNA damage. *Cancer Cell.* 2007;11:175–89.
- Zhang L, Hsu JI, Braekeleer ED, Chen CW, Patel TD, Martell AG, et al. SOD1 is a synthetic-lethal target in *PPM1D*-mutant leukemia cells. *eLife.* 2024;12.
- Beerman I, Seita J, Inlay MA, Weissman IL, Rossi DJ. Quiescent hematopoietic stem cells accumulate DNA damage during aging that is repaired upon entry into cell cycle. *Cell Stem Cell.* 2014;15:37–50.
- Unnikrishnan A, Papaemmanuil E, Beck D, Deshpande NP, Verma A, Kumari A, et al. Integrative Genomics Identifies the Molecular Basis of Resistance to Azacitidine Therapy in Myelodysplastic Syndromes. *Cell Rep.* 2017;20:572–85.
- Johnson JL, Yaron TM, Huntsman EM, Kerelsky A, Song J, Regev A, et al. An atlas of substrate specificities for the human serine/threonine kinase. *Nature.* 2023;613:759–66.
- Palii SS, Van Emburgh BO, Sankpal UT, Brown KD, Robertson KD. DNA methylation inhibitor 5-Aza-2'-deoxycytidine induces reversible genome-wide DNA damage that is distinctly influenced by DNA methyltransferases 1 and 3B. *Mol Cell Biol.* 2008;28:752–71.
- Pappalardi MB, Keenan K, Cockerill M, Kellner WA, Stowell A, Sherk C, et al. Discovery of a first-in-class reversible DNMT1-selective inhibitor with improved tolerability and efficacy in acute myeloid leukemia. *Nat Cancer.* 2021;2:1002–17.
- Wong TN, Ramsingh G, Young AL, Miller CA, Touma W, Welch JS, et al. Role of *TP53* mutations in the origin and evolution of therapy-related acute myeloid leukaemia. *Nature.* 2015;518:552–5.
- Bondar T, Medzhitov R. p53-mediated hematopoietic stem and progenitor cell competition. *Cell stem cell.* 2010;6:309–22.
- Bernstein N, Spencer Chapman M, Nyamondo K, Chen Z, Williams N, Mitchell E, et al. Analysis of somatic mutations in whole blood from 200,618 individuals identifies pervasive positive selection and novel drivers of clonal hematopoiesis. *Nat Genet.* 2024.

42. Emori C, Boucher Z, Bolcun-Filas E. CHEK2 signaling is the key regulator of oocyte survival after chemotherapy. *Sci Adv.* 2023;9:eadg0898.

43. Bolcun-Filas E, Rinaldi VD, White ME, Schimenti JC. Reversal of female infertility by Chk2 ablation reveals the oocyte DNA damage checkpoint pathway. *Science.* 2014;343:533–6.

44. Janiszewska H, Bak A, Hartwig M, Kuliszewicz-Janus M, Calbecka M, Jazwiec B, et al. The germline mutations of the CHEK2 gene are associated with an increased risk of polycythaemia vera. *Br J Haematol.* 2016;173:150–2.

45. Janiszewska H, Bak A, Pilarska M, Heise M, Junkiert-Czarnecka A, Kuliszewicz-Janus M, et al. A risk of essential thrombocythemia in carriers of constitutional CHEK2 gene mutations. *Haematologica.* 2012;97:366–70.

46. Janiszewska H, Bak A, Skonieczka K, Jaskowiec A, Kielbinski M, Jachalska A, et al. Constitutional mutations of the CHEK2 gene are a risk factor for MDS, but not for de novo AML. *Leuk Res.* 2018;70:74–8.

47. Stubbins RJ, Arnovitz S, Vagher J, Asom A, Perpich M, Pies M, et al. Predisposition to hematopoietic malignancies by deleterious germline CHEK2 variants. *Leukemia.* 2025.

48. Thompson DJ, Genovese G, Halvardson J, Ulirsch JC, Wright DJ, Terao C, et al. Genetic predisposition to mosaic Y chromosome loss in blood. *Nature.* 2019;575:652–7.

49. Smith A, Watson N, Sharma P. Frequency of trisomy 15 and loss of the Y chromosome in adult leukemia. *Cancer Genet Cytogenet.* 1999;114:108–11.

50. Zhang Q, Zhao L, Yang Y, Li S, Liu Y, Chen C. Mosaic loss of chromosome Y promotes leukemogenesis and clonal hematopoiesis. *JCI Insight.* 2022;7.

51. Grozdea J, Kessous A, Colombies P. Leukaemia and loss of Y chromosome. *Lancet.* 1973;2:506.

52. Stomper J, Rotondo JC, Greve G, Lubbert M. Hypomethylating agents (HMA) for the treatment of acute myeloid leukemia and myelodysplastic syndromes: mechanisms of resistance and novel HMA-based therapies. *Leukemia.* 2021;35:1873–89.

53. Kim K, Maiti A, Loghavi S, Pourebrahim R, Kadia TM, Rausch CR, et al. Outcomes of TP53-mutant acute myeloid leukemia with decitabine and venetoclax. *Cancer.* 2021;127:3772–81.

54. Muller-Thomas C, Rudelius M, Rondak IC, Haferlach T, Schanz J, Huberle C, et al. Response to azacitidine is independent of p53 expression in higher-risk myelodysplastic syndromes and secondary acute myeloid leukemia. *Haematologica.* 2014;99:e179–81.

55. Middeke JM, Teipel R, Rollig C, Stasik S, Zebisch A, Sill H, et al. Decitabine treatment in 311 patients with acute myeloid leukemia: outcome and impact of TP53 mutations – a registry based analysis. *Leuk Lymphoma.* 2021;62:1432–40.

56. Bally C, Ades L, Renneville A, Sebert M, Eclache V, Preudhomme C, et al. Prognostic value of TP53 gene mutations in myelodysplastic syndromes and acute myeloid leukemia treated with azacitidine. *Leuk Res.* 2014;38:751–5.

57. Jung SH, Kim YJ, Yim SH, Kim HJ, Kwon YR, Hur EH, et al. Somatic mutations predict outcomes of hypomethylating therapy in patients with myelodysplastic syndrome. *Oncotarget.* 2016;7:55264–75.

58. Takahashi K, Patel K, Bueso-Ramos C, Zhang J, Gumbs C, Jabbour E, et al. Clinical implications of TP53 mutations in myelodysplastic syndromes treated with hypomethylating agents. *Oncotarget.* 2016;7:14172–87.

59. Schimmer RR, Kovtonyuk LV, Klemm N, Fullin J, Stoltz SM, Mueller J, et al. TP53 mutations confer resistance to hypomethylating agents and BCL-2 inhibition in myeloid neoplasms. *Blood Adv.* 2022;6:3201–6.

60. Welch JS, Pett AA, Miller CA, Fronick CC, O'Laughlin M, Fulton RS, et al. TP53 and Decitabine in Acute Myeloid Leukemia and Myelodysplastic Syndromes. *N Engl J Med.* 2016;375:2023–36.

ACKNOWLEDGEMENTS

D.N. was supported by the National Institutes of Health (NIH, R01CA193235, R01CA255813, and P01CA265748). D.N. is a Scholar of the Leukemia and Lymphoma

Society. DN was supported by the Henry and Emma Meyer Professorship in Molecular Genetics. Flow cytometry was partially supported by the CPRIT Core Facility Support Award (RP180672) and the NIH (CA125123 and RR024574).

AUTHOR CONTRIBUTIONS

JZ performed most of the experiments with assistance from TH, SL, ML, and XS. DL performed bioinformatics analysis. JZ and DN designed experiments and wrote the manuscript. DN obtained the research fund and administered the study. All authors commented on the manuscript.

COMPETING INTERESTS

The authors declare no competing interests.

ETHICS APPROVAL AND CONSENT TO PARTICIPATE

All methods were performed in accordance with the relevant guidelines and regulations. The animal experiments were approved by BCM Institutional Animal Care and Use Committees (protocol #AN-5858). The study does not include human participants.

ADDITIONAL INFORMATION

Supplementary information The online version contains supplementary material available at <https://doi.org/10.1038/s41375-025-02850-w>.

Correspondence and requests for materials should be addressed to Daisuke Nakada.

Reprints and permission information is available at <http://www.nature.com/reprints>

Publisher's note Springer Nature remains neutral with regard to jurisdictional claims in published maps and institutional affiliations.



Open Access This article is licensed under a Creative Commons Attribution-NonCommercial-NoDerivatives 4.0 International License, which permits any non-commercial use, sharing, distribution and reproduction in any medium or format, as long as you give appropriate credit to the original author(s) and the source, provide a link to the Creative Commons licence, and indicate if you modified the licensed material. You do not have permission under this licence to share adapted material derived from this article or parts of it. The images or other third party material in this article are included in the article's Creative Commons licence, unless indicated otherwise in a credit line to the material. If material is not included in the article's Creative Commons licence and your intended use is not permitted by statutory regulation or exceeds the permitted use, you will need to obtain permission directly from the copyright holder. To view a copy of this licence, visit <http://creativecommons.org/licenses/by-nc-nd/4.0/>.

© The Author(s) 2025